J. Appl. Glycosci., **63**, 7−11 (2016)
doi:10.5458/jag.jag. JAG-2015_019

Regular Paper

A Surface Loop in the N-Terminal Domain of *Pedobacter heparinus* Heparin Lyase II is Important for Activity

(Received July 24, 2015; Accepted September 15, 2015)
(J-STAGE Advance Published Date: September 30, 2015)

Marina Mori,[1] Megumi Ichikawa,[1] Yumiko Kiguchi,[1] Takatsugu Miyazaki,[1] Makoto Hattori,[1] Atsushi Nishikawa,[1] and Takashi Tonozuka[1, †]

[1]*Department of Applied Biological Science, Tokyo University of Agriculture and Technology* (*3−5−8 Saiwai-cho, Fuchu, Tokyo 183−8509, Japan*)

Abstract: *Pedobacter heparinus* heparin lyase II (*Ph*HepII) is composed of N-terminal, central, and C-terminal domains. A long surface loop, designated loop-A, is in the N-terminal domain and is composed of amino acids 84−89. In this study, we deleted two, three, or four residues in loop-A to create Δ86−87, Δ85−87, and Δ84−87 *Ph*HepII deletion mutants. We hypothesized that the deletions would increase *Ph*HepII thermostability. After heating purified *Ph*HepII enzymes at 45 ˚C for 5 min, 6.1 % of the enzyme activity remained in wild-type *Ph*HepII, whereas 10.6 % of the enzyme activity remained in Δ86−87 *Ph*HepII. The results indicated that the deletion caused a significant decrease in the activity, although Δ86−87 *Ph*HepII is slightly more thermostable than wild-type *Ph*HepII. In addtion, Δ85−87 and Δ84−87 *Ph*HepII had weak or no enzyme activity, even when unheated. Circular dichroism spectra showed that Δ85−87 *Ph*HepII was properly folded. These results suggest that the flexibility of loop-A is important for *Ph*HepII enzyme activity.

Key words: heparin lyase, PL21, *Pedobacter heparinus*, thermostability, surface loop, mutagenesis

INTRODUCTION

The polysaccharides heparin and heparan sulfate are classified as glycosaminoglycans and are composed of heterogeneously sulfated repeating disaccharides of iduronic acid (or glucuronic acid) and glucosamine.[1)] The degree of sulfation is higher for heparin than for heparan sulfate. Heparin lyases degrade heparin and heparan sulfate via a β-elimination mechanism.[2,3)] Three types of heparin lyases, HepI, HepII, and HepIII, have been identified. HepI primarily degrades heparin (EC 4.2.2.7), and HepIII primarily degrades heparan sulfate (EC 4.2.2.8), but HepII degrades both heparin and heparan sulfate.[4,5)] According to the carbohydrate-active enzymes database (CAZy),[6)] HepI, HepII, and HepIII belong to polysaccharide lyase families PL13, PL21, and PL12, respectively.

Pedobacter heparinus (formerly known as *Flavobacterium heparinum*) HepII (*Ph*HepII) efficiently cleaves the glucosamine-uronic acid linkages in heparin and heparan sulfate to produce unsaturated oligosaccharides.[7)] The crystal structure of *Ph*HepII has been determined.[8,9)] *Ph*HepII forms a homodimer, and each subunit is composed of an N-terminal, a central, and a C-terminal domain (Fig. 1). The N-terminal domain is α-helical, whereas the central and C-terminal domains are primarily composed of β-strands. Based on the structure of the *Ph*HepII-disaccharide complex, a deep cleft formed by the N-terminal and central domains has been identified as the catalytic cleft.[8)]

There is a long loop, designated here loop-A, consisting of amino acids 84−89 (Trp-Lys-Pro-Ala-Asp-Ile) in the N-terminal domain of *Ph*HepII at the entrance of the catalytic cleft. In some enzymes, shortening of the surface loop has been reported to enhance enzymatic activity and/or stability.[10,11)] Loop-A is located relatively far (~20 Å) from the catalytic cleft and does not appear to interact with the substrate (Fig. 1A). The modification of residues with high *B* values increases thermostability in some proteins.[12,13)] In the crystal structure of the *Ph*HepII (PDB ID, 2FUQ)[8)], the average *B* value of all of the amino acid residues is 29.4 Å^2, whereas that of the amino acid residues within loop-A is 40.3 Å^2, which is the highest *B* values in *Ph*HepII. Also, conserved amino acid residues generally play a critical role in the activity.[14)] According to the CAZy database, 10 genes have been classified as PL21 lyases, and the sequences were aligned using the Clustal Omega server[15)] (http://www.ebi.ac.uk/Tools/msa/clustalo/) (Fig. 1B). The sequence alignment of the PL21 lyases shows that only *Ph*HepII possesses the loop-A WKPADI sequence. Therefore, we predicted that shortening loop-A would enhance *Ph*HepII thermostability without loss of the activity. In this study, two, three, or four residues were deleted from loop-A to create the mutants Δ86−87, Δ85−87, and 84−87 and determine whether shortening loop-A increases the thermostability of *Ph*HepII.

† Corresponding author (Tel. +81−42−367−5702, Fax. +81−42−367−5705, E-mail: tonozuka@cc.tuat.ac.jp).
Abbreviations: GuHCl, guanidine hydrochloride; Ni-NTA, nickel-nitrilotriacetic acid; *Ph*HepII, *Pedobacter heparinus* heparin lyase II; WT, wild-type.

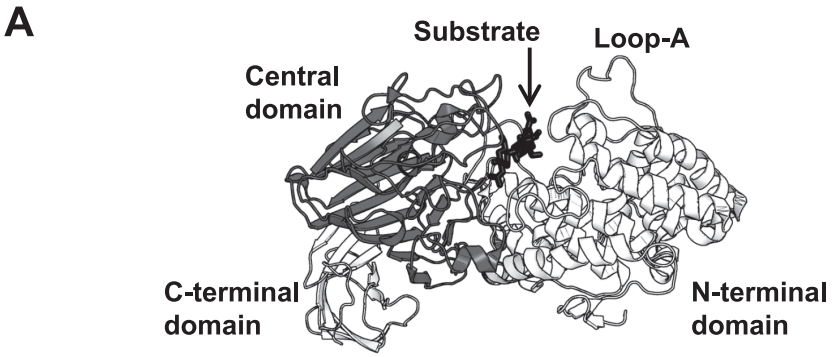

B

```
PhHepII                                  YLREQQVPDLKNRMNDPKLKKVWADMIKMQEDWKPADIPEV--KDFRFYFNQKGLTVRVE
Bacteroides eggerthii 01675              YVRSSDLPVLKERMKTPQAQQTLSLMKELGKDRTPDEEAAVTNRGFRYYYEMRGVTTRVQ
Bacteroides stercoris ATCC43183 00262    YVRSSDLPALKERLKTPQAQQTLSLMKELSKDRTPAEEAAVTNRGFRYYYEMRGVTSRVQ
Bacteroides intestinalis 00904           YVRPANLPDLKKRMDHPQVKANLATLRKLGIDRTAEEEAKVTDRGFRYYFEMRGVTSRVQ
Bacteroides eggerthii 03043              YVRSADLPDLKKRMNHPHVKEVLATLNKLGKDRTPEEEAKVKDRGFRYYFEMRGVTSRVQ
Bacteroides stercoris ATCC43183 02129    YVRSADLPDLKKRMEHPHVKEVLATLNKLGKDRTPEEEAKVKDRGFRYYFEMRGVTSRVQ
Bacteroides stercoris HJ-15              YVRSADLPDLKKRMEHPHVKEVLATLNKLGKDRTPEEEAKVKDRGFRYYFEMRGVTSRVQ
Victivallis vadensis 0838                WVTPESLPQVRANLTAPENRAAWEFIRREAAKPVAF-----KADSGREVTPEPAVLKAAA
Niastella koreensis 3778                 WVTPAFLPVLKERIQAAENNTAWNKVQQTALTDYPF-----TPDTTKEIFYNEQLENIIR
Pedobacter saltans 0684                  WVNSESLPIVKSRLEKGENKAYWEKVKNSALRPFEF-----KFDPKEEVAFNEELEKAAE
                                         ::    :* :: .:   . .    : .                .       :
```

Fig. 1. Structure of *Ph*HepII and sequence alignment with other PL21 proteins.

(A) Crystal structure of *Ph*HepII. A monomer of *Ph*HepII is shown. N-terminal, central, and C-terminal domains are indicated by different gray levels. The image was generated using PDB ID 3E7J, and the program PyMol (http://www.pymol.org/). (B) Sequence alignment of PL21 lyases, including *Ph*HepII. Alignment was performed using the Clustal Omega server (http://www.ebi.ac.uk/Tools/msa/clustalo/). The loop-A sequence (residues 84−89) in *Ph*HepII is underlined.

MATERIALS AND METHODS

Plasmid construction. *P. heparinus* NBRC 12017 was obtained from the NITE Biological Resource Center (Kisarazu, Japan). *Escherichia coli* strain JM109 was used for DNA manipulations. Wild-type (WT) HepII was cloned into an expression vector as described previously.[8] Briefly, the *Ph*HepII gene was amplified by PCR, and the PCR product was cloned into pET28a (Novagen®; Merck KGaA, Darmstadt, Germany). Site-directed mutagenesis of the resulting plasmid was carried out using the QuikChange Site-Directed Mutagenesis Kit (Agilent Technologies, Inc., Santa Clara, USA). Primers for the construction of the deletion mutants were as follows: Δ86−87, 5′-ATG CAG GAA GAC TGG AAG GAT ATC CCT GAA GTT AAA GAC-3′; Δ85−87, 5′-ATG CAG GAA GAC TGG GAT ATC CCT GAA GTT AAA GAC-3′; and Δ84−87, 5′-C AAG ATG CAG GAA GAC GAT ATC CCT GAA GTT AAA GAC TTT-3′. Primers complementary to these sequences were also used. All constructs were verified by DNA sequencing.

Protein expression and purification. WT and deletion mutant *Ph*HepII expression constructs were transformed into *E. coli* BL21(DE3), and transformants were grown at 37 °C in 200 mL Luria-Bertani (LB) medium containing kanamycin (20 μg/mL) to A_{600} = 0.6 to 0.8. Cells were then induced with 0.5 mM isopropyl β-D-thiogalactoside and further cultivated at 30 °C for 18 h. Cells were harvested by centrifugation at 5,000 × G for 5 min, resuspended in 8 mL of 50 mM Tris-HCl (pH 7.5), and lysed by sonication. Lysed cells were centrifuged at 12,000 × G for 20 min, and the supernatant was applied onto a 5-mL column (diameter of 2.5 cm) containing nickel-nitrilotriacetic acid (Ni-NTA) agarose (Qiagen GmbH, Hilden, Germany). The column was equilibrated with 50 mM Tris-HCl and 0.5 M sodium chloride (buffer A), and the enzyme was eluted with 30 mL buffer A containing 50 mM imidazole (Fig. 2). The eluted fractions were collected and the original buffer was replaced with 50 mM sodium phosphate buffer (pH 7.0) using an Amicon Ultracell-30K centrifugal filter unit (Merck Millipore, Darmstadt, Germany).

Enzymatic activity. The substrate solution consisted of 70 μL heparin (10 mg/mL; Wako Pure Chemical Industries, Osaka, Japan) from pig intestinal mucosa and 560 μL buffer (0.01 % bovine serum albumin and 50 mM sodium phosphate, pH 7.0). Seventy microliters of enzyme (0.25 mg/mL in 50 mM sodium phosphate, pH 7.0; final concentration, 25 μg/mL) was added to the substrate solution to start the reaction, and the reaction was incubated at 25 °C. Aliquots (100 μL) were taken at 10 min or 5-min intervals and mixed with 1 mL of 60 mM HCl to stop the reaction. Absorbances at 232 nm were then measured. Each measurement was performed at least three times. Activity was calculated using a molar extinction coefficient of 3,800 M^{-1} cm^{-1} for unsaturated oligosaccharides.[16] One unit (U) of activity was defined as the amount of enzyme that liberated 1 μmol unsaturated oligosaccharide per minute. Protein concentrations were determined by measuring the absorbance at 280 nm, and the molar extinction coefficient (1 mg/mL solution of WT, Δ86−87, and Δ85−87, = 1.60; 1 mg/mL solution of Δ84−87 = 1.54) was calculated using the Expasy ProtParam server (http://web.expasy.org/protparam/).

Circular dichroism (CD) spectroscopy. CD spectra were obtained for WT and mutant enzymes (0.1 mg/mL) using a

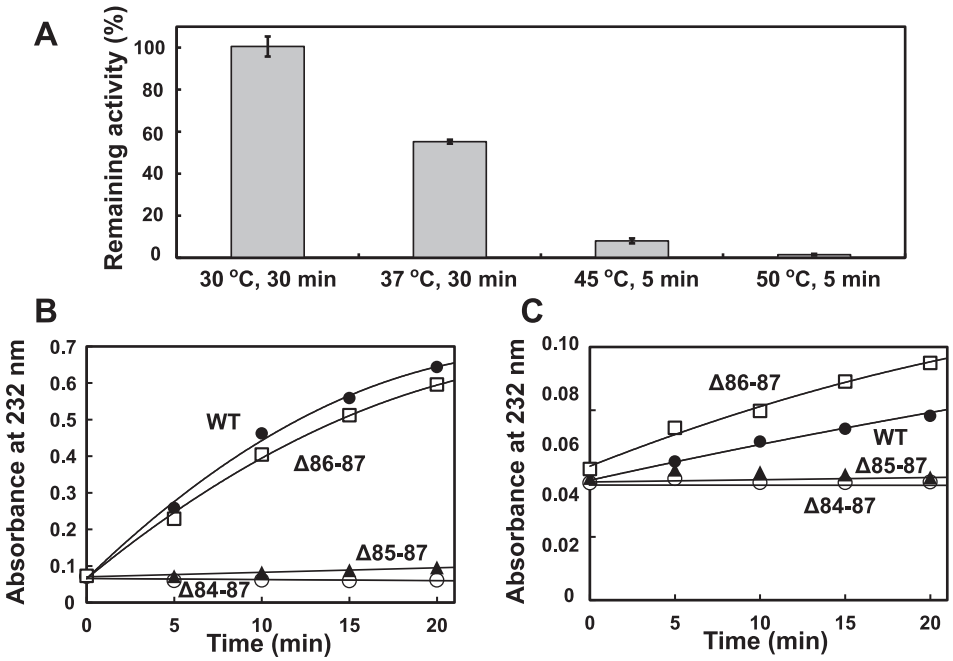

Fig. 2. Enzymatic activity and thermostability of *Ph*HepII.

(A) Thermostability of WT *Ph*HepII. The enzyme was incubated under the indicated conditions, and the remaining activities were assayed at 25 ˚C for 10 min. The activity of unheated enzyme was calculated as 100 %. Bars represent the mean ± standard deviation. (B, C) Time course of product formation by unheated (B) and heat-treated (C) enzymes (25 μg/mL). Black circle, WT *Ph*HepII; white square, Δ86−87 *Ph*HepII; black triangle, Δ85−87 *Ph*HepII; white circle, Δ84−87 *Ph*HepII.

0.1-cm cell in a JASCO J720WI spectrometer (JASCO Corporation, Tokyo, Japan) at 20 ˚C. Five spectra from 200−250 nm were taken at a scan speed of 50 nm/min with a bandwidth of 1 nm and averaged for each sample; buffer spectra were subtracted.

RESULTS

Purification of WT and mutant PhHepII.

WT, Δ86−87, Δ85−87, and Δ84−87 *Ph*HepII were purified to homogeneity (Fig. S1; See J. Appl. Glycosci. Web site). In the purification of Δ86−87, Δ85−87, and Δ84−87, a small amount of *Ph*HepII proteins was contained in the flow-through fractions (lanes 3 in Fig. S1; See J. Appl. Glycosci. Web site), but all the fractions eluted with buffer A containing 50 mM imidazole were observed as a single band on SDS-PAGE (lanes 4 in Fig. S1; See J. Appl. Glycosci. Web site). The eluted fractions were collected and used as the purified *Ph*HepII.

Enzymatic activities and CD spectra of WT and mutant PhHepII.

We first investigated the thermostability of WT *Ph*HepII under the condition used in this work. The enzyme (0.25 mg/mL) was incubated at various temperatures for 5 min or 30 min and the remaining activities were assayed at 25 ˚C for 10 min (Fig. 2A). About a half of the activity was remained when incubated at 37 ˚C for 30 min, but the activity was markedly decreased above 45 ˚C, and the remaining activity at 45 ˚C for 5 min was 6 %. A similar observation has been reported for the thermostability of *Bacteroides stercoris* HJ-15 HepII (58 % identity), which lose its activity rapidly above 40 ˚C.[5)]

The enzymatic activities of WT, Δ86−87, Δ85−87, and Δ84−87 *Ph*HepII were determined by measuring product formation over time (Fig. 2B). When analyzed graphically, product formation was not linear but fit a square regression, probably because the substrate concentration decreased as the enzymatic reaction proceeded, leading to the deceleration of substrate degradation. Specific activities were calculated from three separate experiments (Table 1), and the specific activity of Δ86−87 *Ph*HepII (3.93 ± 0.25 U/mg) was lower than that of WT (5.22 ± 0.26 U/mg). The activity of Δ85−87 was almost lost, and no enzymatic activity was detected for Δ84−87.

To determine the thermostabilities of WT and mutant *Ph*HepII enzymes, the enzymes were incubated at 45 ˚C for 5 min, and their specific and residual enzymatic activities were measured (Fig. 2C). Although the activities were low, the plots were well fit to the regression curves, indicating that the activities were accurately measured. The specific activity of heat-treated Δ86−87 *Ph*HepII (0.415 ± 0.034 U/mg) was slightly higher than that of WT (0.318 ± 0.044 U/mg) (Table 1). The residual enzymatic activities of WT and Δ86−87 *Ph*HepII were 6.1 and 10.6 %, respectively.

Far-UV CD spectra of WT, Δ86−87, and Δ85−87 *Ph*HepII from 200−250 nm were analyzed to determine whether these

Table 1. Specific activities of wild-type and deletion mutants of *Ph*HepII.

Enzyme	No treatment (U/mg)	After incubation at 45 ˚C for 5 min (U/mg)
WT	5.22 ± 0.26	0.318 ± 0.044
Δ86−87	3.93 ± 0.25	0.415 ± 0.034
Δ85−87	0.130 ± 0.035	ND[a]
Δ84−87	ND[a]	ND[a]

[a]ND, not detected.

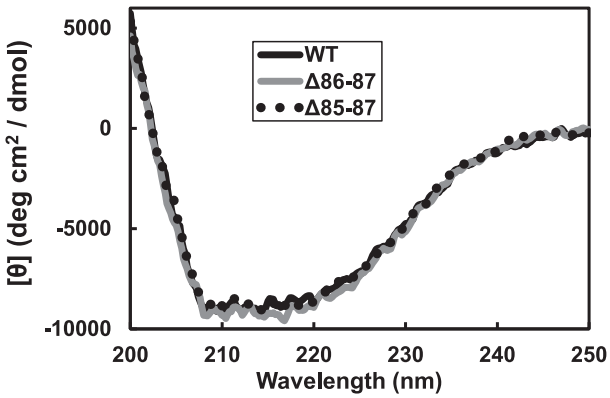

Fig. 3. CD spectra of PhHepII from 200−250 nm.

The enzymes at a concentration of 0.1 mg/mL were analyzed. Solid black line, WT *Ph*HepII; solid gray line, Δ86−87 *Ph*HepII; dotted line, Δ85−87 *Ph*HepII.

mutations affected the folding of *Ph*HepII (Fig. 3). WT and mutant CD spectra were superimposable.

DISCUSSION

In this study, we hypothesized that shortening of loop-A would enhance the thermostability of *Ph*HepII. When the enzymatic activities of unheated WT and Δ86−87 *Ph*HepII were set to 100 %, heating at 45 ˚C for 5 min reduced the activities of WT and Δ86−87 *Ph*HepII to 6.1 and 10.6 %, respectively (Fig. 3, Table 1). This result demonstrates that the thermostability of Δ86−87 *Ph*HepII is slightly higher than that of WT. However, the specific activity of Δ86–87 *Ph*HepII (3.93 U/mg) was 1.3-fold lower than that of WT (5.22 U/mg) and Δ85−87 *Ph*HepII had very weak enzymatic activity (0.130 U/mg) (Table 1) indicating that loop-A is critical for *Ph*HepII activity. The CD spectra of WT, Δ86−87, and Δ85−87 *Ph*HepII were nearly identical indicating that deletion of residues 85−87 did not affect the folding of *Ph*HepII (Fig. 3). While many rational approaches to thermostabilize proteins have been reported to be successful, this study shows that the molecular basis for the increased thermostability is extraordinarily subtle as suggested previously.[13,17] The sequence homology of PL21 proteins around loop-A was low (Fig. 1B), suggesting that the flexibility of the loop, rather than a single residue such as Lys85, is likely to be important for *Ph*HepII activity.

It has been reported that one or two lid loops are present at the entrance of the catalytic cleft in PL5,[18] PL7,[19] and PL18[20] enzymes. The PL5 alginate lyase A1-III from *Sphingomonus* sp. is composed of $(\alpha/\alpha)_6$ barrel, and a lid loop, comprising residues 64−85, extends from the $(\alpha/\alpha)_6$ barrel fold. Crystallography of a PL5 alginate lyase revealed a large conformational change in the lid loop during catalysis, and the maximum movement reaches 13.4 Å. Along with this loop motion, residues located in the loop, Arg67, Tyr68, and Tyr80, interact with the substrate.[18] PL7 and PL16 lyases are composed of β-jelly roll, and a combination of two lid loops has been predicted to oscillate based on a structural comparison[19] and a molecular dynamic simulation.[20] Crystallography results demonstrated that the *B* values of the amino acids in the lid loops of a PL18 alginate lyase were also high.[20] It is unclear whether a similar conformational change occurs in loop-A in *Ph*HepII, but it has been reported that large loop motions may not be observed by protein crystallography due to the influence of crystal packing.[21] Although the overall structure of *Ph*HepII differs from the PL5, PL7, and PL18 alginate lyase structures, the loop-A of *Ph*HepII likely contributes to enzymatic activity in a manner similar to the PL5, PL7, and PL18 lid loops.

REFERENCES

1) L. Kjellén and U. Lindahl: Proteoglycans: structures and interactions. *Annu. Rev. Biochem.,* **60**, 443−475 (1991).
2) R.J. Linhardt, P.M. Galliher, and C.L. Cooney: Polysaccharide lyases. *Appl. Biochem. Biotechnol.,* **12**, 135−176 (1986).
3) M.L. Garron and M. Cygler: Structural and mechanistic classification of uronic acid-containing polysaccharide lyases. *Glycobiology*, **20**, 1547−1573 (2010).
4) R.J. Linhardt, J.E. Turnbull, H.M. Wang, D. Loganathan, and J.T. Gallagher: Examination of the substrate specificity of heparin and heparan sulfate lyases. *Biochemistry,* **29**, 2611−2617 (1990).
5) Y.J. Hyun, K.S. Lee, and D.H. Kim: Cloning, expression and characterization of acharan sulfate-degrading heparin lyase II from *Bacteroides stercoris* HJ-15. *J. Appl. Microbiol.,* **108**, 226−235 (2010).
6) V. Lombard, H. Golaconda Ramulu, E. Drula, P.M. Coutinho, and B. Henrissat: The Carbohydrate-active enzymes database (CAZy) in 2013. *Nucleic Acids Res.,* **42**, D490−D495 (2014).
7) H.B. Nader, M.A. Porcionatto, I.L. Tersariol, M.A. Pinhal, F.W. Oliveira, C.T. Moraes, and C.P. Dietrich: Purification and substrate specificity of heparitinase I and heparitinase II from *Flavobacterium heparinum*. Analyses of the heparin and heparan sulfate degradation products by ^{13}C NMR spectroscopy. *J. Biol. Chem.,* **265**, 16807−16813 (1990).
8) D. Shaya, A. Tocilj, Y. Li, J. Myette, G. Venkataraman, R. Sasisekharan, and M. Cygler: Crystal structure of heparinase II from *Pedobacter heparinus* and its complex with a disaccharide product. *J. Biol. Chem.,* **281**, 15525−15535 (2006).
9) D. Shaya, W. Zhao, M.L. Garron, Z. Xiao, Q. Cui, Z. Zhang, T. Sulea, R.J. Linhardt, and M. Cygler: Catalytic mechanism of heparinase II investigated by site-directed mutagenesis and the crystal structure with its substrate. *J. Biol. Chem.,* **285**, 20051−20061 (2010).
10) A. Meinke, H.G. Damude, P. Tomme, E. Kwan, D.G. Kilburn, R.C. Miller Jr, R.A. Warren, and N.R. Gilkes: Enhancement of the endo-β-1,4-glucanase activity of an exocellobiohydrolase by deletion of a surface loop. *J. Biol. Chem.,* **270**, 4383−4386 (1995).
11) M.J. Thompson and D. Eisenberg: Transproteomic evidence of a loop-deletion mechanism for enhancing protein thermostability. *J. Mol. Biol.,* **290**, 595−604 (1999).
12) M.T. Reetz, J.D. Carballeira, and A. Vogel: Iterative saturation mutagenesis on the basis of *B* factors as a strategy for increasing protein thermostability. *Angew. Chem. Int. Ed. Engl.,* **45**, 7745−7751 (2006).
13) Y. Ohta, Y. Hatada, Y. Hidaka, Y. Shimane, K. Usui, T. Ito, K. Fujita, G. Yokoi, M. Mori, S. Sato, T. Miyazaki, A. Nishikawa, and T. Tonozuka: Enhancing thermostability and the structural characterization of *Microbacterium saccharophilum* K-1 β-fructofuranosidase. *Appl. Microbiol. Biotechnol.,* **98**, 6667−6677 (2014).
14) A.M. Poole and R. Ranganathan: Knowledge-based potentials in protein design. *Curr. Opin. Struct. Biol.*, **16**, 508−513 (2006).
15) H. McWilliam, W. Li, M. Uludag, S. Squizzato, Y.M. Park, N. Buso, A.P. Cowley, and R. Lopez: Analysis Tool Web Services from the EMBL-EBI. *Nucleic Acids Res.,* **41**, W597−W600 (2013).
16) D.L. Lohse and R.J. Linhardt: Purification and characterization of heparin lyases from *Flavobacterium heparinum*. *J. Biol. Chem.,* **267**, 24347−24355 (1992).
17) C. Dumon, A. Varvak, M.A. Wall, J.E. Flint, R.J. Lewis, J.H. Lakey, C. Morland, P. Luginbühl, S. Healey, T. Todaro, G. DeSantis, M. Sun, L. Parra-Gessert, X. Tan, D.P. Weiner, and H.J. Gilbert: Engineering hyperthermostability into a GH11 xylanase is mediated by subtle changes to protein structure. *J. Biol. Chem.,*

283, 22557−22564 (2008).
18) B. Mikami, M. Ban, S. Suzuki, H.J. Yoon, O. Miyake, M. Yamasaki, K. Ogura, Y. Maruyama, W. Hashimoto, and K. Murata: Induced-fit motion of a lid loop involved in catalysis in alginate lyase A1-III. *Acta Crystallogr. D Biol. Crystallogr.,* **68**, 1207−1216 (2012).
19) M. Yamasaki, K. Ogura, W. Hashimoto, B. Mikami, and K. Murata: A structural basis for depolymerization of alginate by polysaccharide lyase family-7. *J. Mol. Biol.*, **352**, 11−21 (2005).
20) S. Dong, T.D. Wei, X.L. Chen, C.Y. Li, P. Wang, B.B. Xie, Q.L. Qin, X.Y. Zhang, X.H. Pang, B.C. Zhou, and Y.Z. Zhang: Molecular insight into the role of the N-terminal extension in the maturation, substrate recognition, and catalysis of a bacterial alginate lyase from polysaccharide lyase family 18. *J. Biol. Chem.,* **289**, 29558−29569 (2014).
21) M. Tamura, T. Miyazaki, Y. Tanaka, M. Yoshida, A. Nishikawa, and T. Tonozuka: Comparison of the structural changes in two cellobiohydrolases, CcCel6A and CcCel6C, from *Coprinopsis cinerea* - a tweezer-like motion in the structure of CcCel6C. *FEBS J.,* **279**, 1871−1882 (2012).